# Simulations of the Effect of Gas Drag on the Dynamics of Spherical Bodies in the Primordial Solar Nebula

Christopher J. Stawarz

August 19, 1999

## 1 Introduction

Tracing the origin of the planets from the primordial solar gas cloud has long proved problematic for astrophysicists. Recent discoveries of extrasolar planetary systems have provided new observational evidence with which to evaluate general theories of planet formation and have lead to some revisions in these theories (see, for example, Refs. [1, 2]). However, the exact physical processes that caused the primordial solar nebula to evolve into the system of planets, satellites, and smaller bodies present today remain poorly understood.

Recent studies have attempted to trace the evolution of planetesimals from bodies with radii on the order of 100 m to moon-size (1000 km) bodies via gravitational N-body simulations [3, 4]. These simulations have been conducted under the assumption that the drag force exerted by the nebula gas has a negligible effect on the dynamics of bodies in the size range of interest. Although this appears to be a reasonable assumption, a thorough computational analysis of the effects of drag on bodies in the solar nebula is necessary to assure its validity.

In order to obtain a better understanding of the effects of gas drag on planetesmials, we have simulated the dynamical evolution of bodies of various sizes and densities orbiting the Sun in solar nebulas of varying density. In Section 2, we give an overview of the models of the solar nebula and drag force that we have employed. In Section 3, we present, for comparison, previous theoretical predictions of the effect of gas drag on planetesimal dynamics. Section 4 contains the results of our simulations and discusses the general trends that can be extracted from them and how these compare with those expected from theory. Finally, Section 5 discusses future applications of our code that would provide insight into some of the subtler effects of gas drag.

## 2 Model

### 2.1 Solar Nebula

We have employed the model of the solar nebula first proposed by Kusaka, Nakano, and Hayashi [5] and later extended by Adachi, Hayashi, and Nakazawa [6] and Hayashi [7]. This model and variations on it have been used extensively in studies of the dynamics of bodies in the early solar system (for example, see Refs. [8, 9, 10]). In this model, the nebula is a disk composed primarily of hydrogen molecules that is in circular motion around the Sun. The angular velocity of the gas is slightly different than its predicted Keplerian angular velocity because of a radial pressure gradient. Employing a heliocentric cylindrical coordinate system where $z = 0$ corresponds to the equatorial plane of the Sun, Hayashi [7] gives equations for the density and temperature of the gas of

$$\rho(r,z) = \rho_0 r^{-2.75} \exp\left\{-\frac{1}{2}\left(\frac{z\omega_K}{c}\right)^2\right\}$$

$$T(r) = T_0 r^{-1/2}$$

where $r$ is in AU, $\rho_0 = 1.4\times10^{-9}\,\mathrm{g/cm^3}$, $T_0 = 280\,\mathrm{K}$, and $c$ and $\omega_K$ are the sound velocity in the gas at $(r,z)$ and the Keplerian angular velocity of a solid body at $r$, respectively. The angular velocity of the gas is given by [6]

$$\omega_g(r,z) = \omega_k(r)\{1 - 2\eta(r,z)\}^{1/2}$$

where $\eta(r,z)$ depends on the radial pressure gradient of the gas and has the form

$$\eta(r,z) = \frac{\pi}{16}\left[3.25 - 1.25\left(\frac{z\omega_K}{c}\right)^2\right]\left(\frac{c_m}{v_K}\right)^2$$

Here, $c_m$ is the mean thermal velocity of the gas molecules and $v_K$ is the Keplerian velocity corresponding to $\omega_K$.

## 2.2 Drag Force

The general form for the drag force on a spherical body moving through a gas is

$$f_D = \frac{1}{2}C_D \pi r_p^2 \rho u^2$$

where $r_p$ is the radius of the body, $u$ is the relative velocity of the body with respect to the gas, $\rho$ is the density of the gas, and $C_D$ is the dimensionless drag coefficient. In general, the drag coefficient is a function of the Mach, Knudsen, and/or Reynolds numbers of the body. However, we have followed Adachi et al. [6] and employed four special cases where $C_D$ has a fairly simple form. These are summarized below. ($\mu$ is the viscosity of the gas.)

$$\begin{aligned}
M \gg 1 \quad &\Rightarrow \quad f_D = \pi r_p^2 \rho u^2 \\
M \ll 1, K > 1 \quad &\Rightarrow \quad f_D = \frac{4\pi}{3} r_p^2 \rho c_m u \\
M \ll 1, K < 1, R_e \lesssim 10 \quad &\Rightarrow \quad f_D = 6\pi\mu r_p u \\
M \ll 1, K \ll 1, R_e \gtrsim 10^3 \quad &\Rightarrow \quad f_D = 0.25\pi r_p^2 \rho u^2
\end{aligned}$$

For intermediate cases, we have interpolated between these limiting cases. This method has proved sufficient to cover the full ranges of $M$, $K$, and $R_e$ encountered in our study.

# 3 Theoretical Predictions

For comparison with the results of our simulations, we first present the theoretical predictions of Adachi et al. regarding the decay time of the semimajor axis of a body initially at 1 AU from the Sun and possessing the corresponding Keplerian velocity. Adaci et al. have calculated the decay time in years for such a body to be [6]

$$\tau = 80\left(\frac{1+g^2}{2g}\right)$$

where

$$g = \frac{f_D}{mu\omega_K}$$

and $m$ is the mass of the body. The values of $\tau$ for gas densities with $\rho_0 = 10^{-8}$, $10^{-9}$, and $10^{-10}\,\mathrm{g/cm^3}$; particle radii $r_p = 1$ to $10^6\,\mathrm{m}$; and particle densities $\rho_p = 1$, 2, and $3\,\mathrm{g/cm^3}$ are shown in Figures 1, 2, and 3. From these results, we find that, as expected, the decay time increases with increasing particle radius and density and decreasing gas density. Note that the initial, more highly sloped region of each graph corresponding to the smallest particle radii is independent of the gas density.

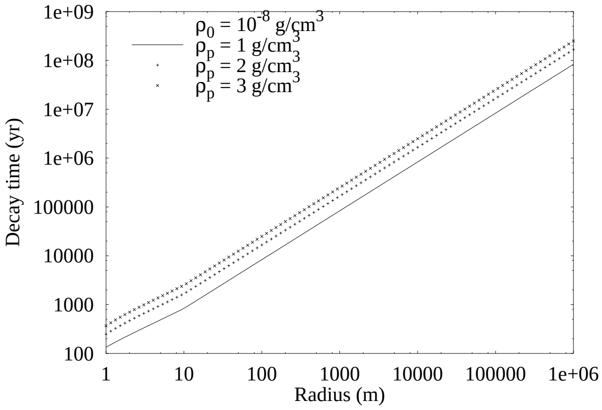


Figure 1: Predicted decay time of the semimajor axis for spherical bodies initially at 1 AU from the Sun with the corresponding Keplerian velocity in a nebula with $\rho_0 = 10^{-8}\,\mathrm{g/cm^3}$.

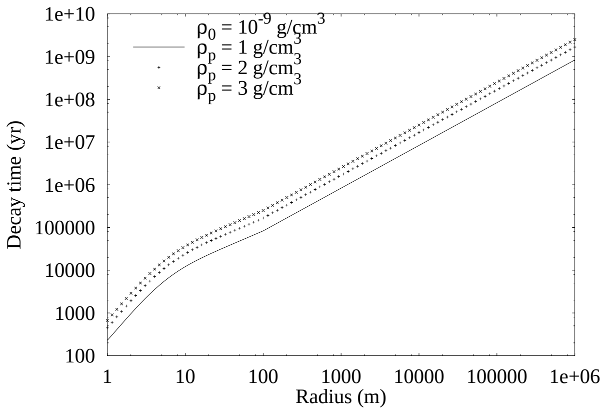


Figure 2: Predicted decay time of the semimajor axis for spherical bodies initially at 1 AU from the Sun with the corresponding Keplerian velocity in a nebula with $\rho_0 = 10^{-9}\,\mathrm{g/cm^3}$.

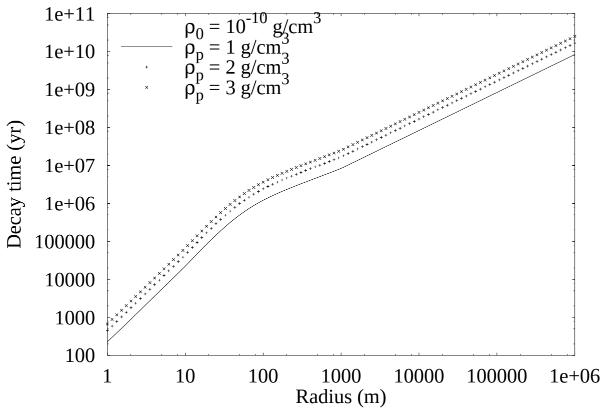


Figure 3: Predicted decay time of the semimajor axis for spherical bodies initially at 1 AU from the Sun with the corresponding Keplerian velocity in a nebula with $\rho_0 = 10^{-10}\,\mathrm{g/cm^3}$.

# 4 Simulation Results

Using the model of the solar nebula described in Section 2.1 and the drag force given in Section 2.2, we have simulated the dynamical evolution of a variety of spherical bodies placed in the nebula at an initial distance of 1 AU from the Sun with the corresponding Keplerian velocity. In the simulations, particles were evolved via the leapfrog algorithm, which, in the case of velocity-dependent acceleration, has the form

$$\begin{aligned}
x_{1/2} &= x_0 + \frac{\tau}{2} v_0 \\
v_{1/2}^{pred} &= v_0 + \frac{\tau}{2} a_{-1/2} \\
v_1 &= v_0 + \tau a(x_{1/2}, v_{1/2}^{pred}) \\
x_1 &= x_{1/2} + \frac{\tau}{2} v_1
\end{aligned}$$

where $\tau$ is the time step. The Sun was implemented as another body, meaning it responded to the gravitational influence of the test body, although the drag force was not applied to it. The center of mass of the system was placed at the origin ($r = z = 0$), and the nebula was centered there. All simulations ran until they reached the minimum number of timesteps per orbit required for accurate integration, which we set at 30. This corresponds to a minimum semimajor axis of

$$a_{min} = \left\{ GM_\odot \left( \frac{15\tau}{\pi} \right)^2 \right\}^{1/3}$$

The results of our simulations are shown in graphs of semimajor axis versus time for various body sizes and densities and gas densities. Figures 4 through 12 show the results for bodies of radius $r_p = 1$, 10, and 100 m in nebulae with gas density prefactors $\rho_0 = 1.4 \times 10^{-8}$, $1.4 \times 10^{-9}$, and $1.4 \times 10^{-10}\,\mathrm{g/cm^3}$. Figs. 13 through 15 show the results for $r_p = 10^3$, $10^4$, and $10^5$ m and $\rho_0 = 1.4 \times 10^{-8}\,\mathrm{g/cm^3}$. Each graph contains the results for body densities of $\rho_p = 1$, 2, and $3\,\mathrm{g/cm^3}$ except for Fig. 15, which shows only the $\rho_p = 1\,\mathrm{g/cm^3}$ case.

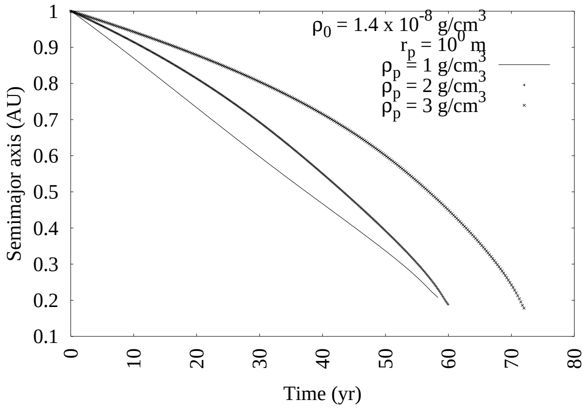


Figure 4: Semimajor axis versus time for bodies of radius $r_p = 10^0\,\mathrm{m}$ in a nebula with $\rho_0 = 10^{-8}\,\mathrm{g/cm^3}$.

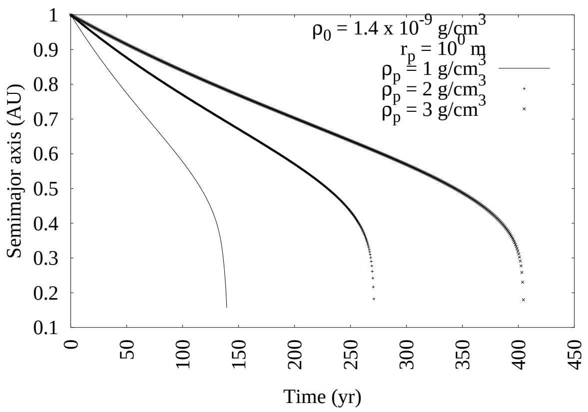


Figure 5: Semimajor axis versus time for bodies of radius $r_p = 10^0\,\mathrm{m}$ in a nebula with $\rho_0 = 10^{-9}\,\mathrm{g/cm^3}$.

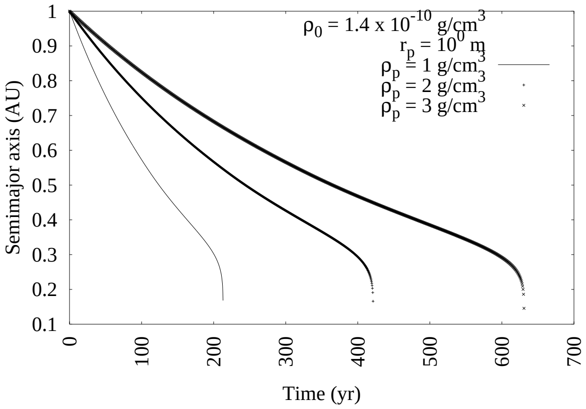


Figure 6: Semimajor axis versus time for bodies of radius $r_p = 10^0\,\mathrm{m}$ in a nebula with $\rho_0 = 10^{-10}\,\mathrm{g/cm^3}$.

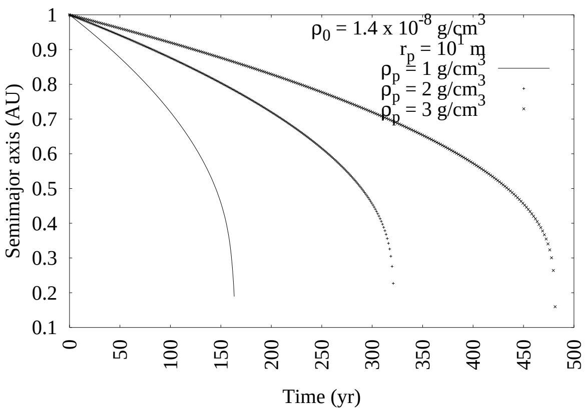


Figure 7: Semimajor axis versus time for bodies of radius $r_p = 10^1\,\mathrm{m}$ in a nebula with $\rho_0 = 10^{-8}\,\mathrm{g/cm^3}$.

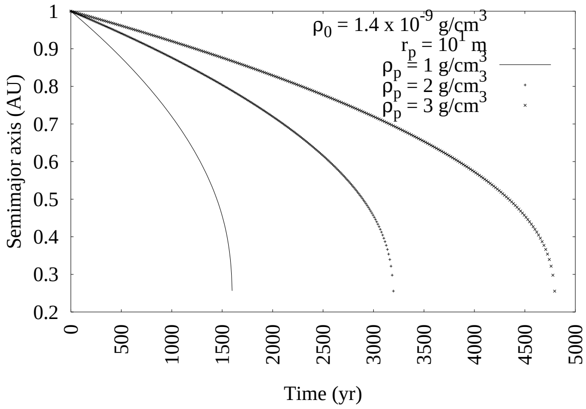


Figure 8: Semimajor axis versus time for bodies of radius $r_p = 10^1$ m in a nebula with $\rho_0 = 10^{-9}$ g/cm$^3$.

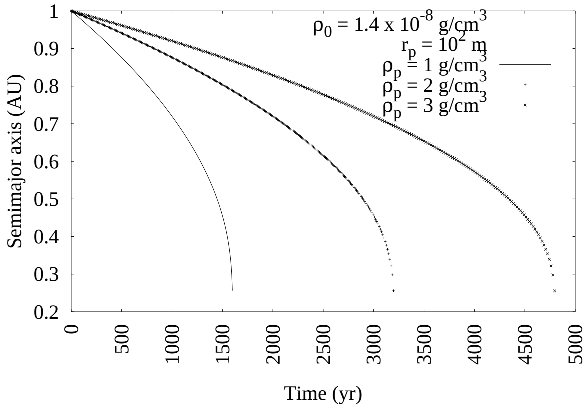


Figure 10: Semimajor axis versus time for bodies of radius $r_p = 10^2$ m in a nebula with $\rho_0 = 10^{-8}$ g/cm$^3$.

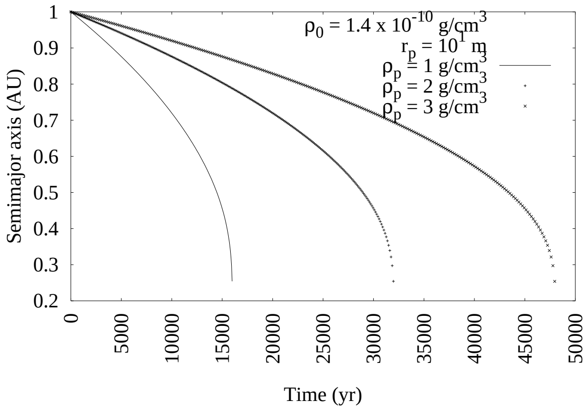


Figure 9: Semimajor axis versus time for bodies of radius $r_p = 10^1$ m in a nebula with $\rho_0 = 10^{-10}$ g/cm$^3$.

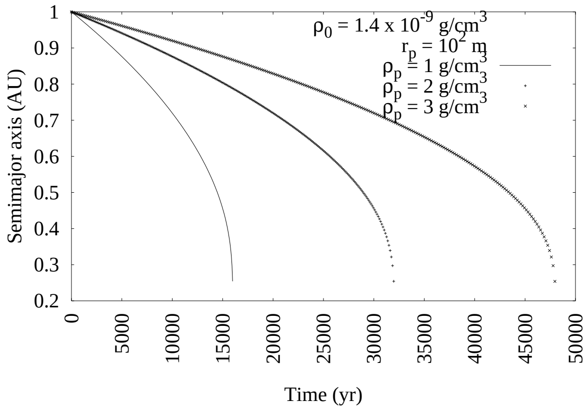


Figure 11: Semimajor axis versus time for bodies of radius $r_p = 10^2$ m in a nebula with $\rho_0 = 10^{-9}$ g/cm$^3$.

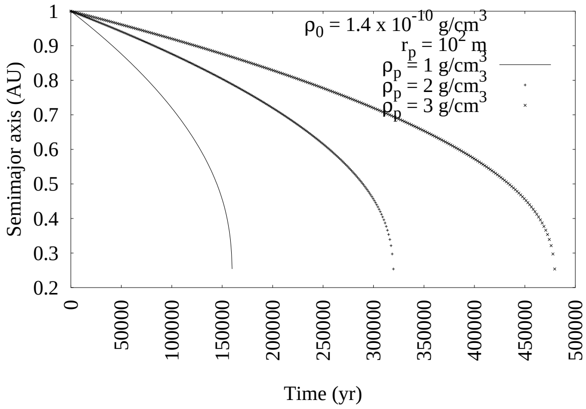


Figure 12: Semimajor axis versus time for bodies of radius $r_p = 10^2\,\mathrm{m}$ in a nebula with $\rho_0 = 10^{-10}\,\mathrm{g/cm^3}$.

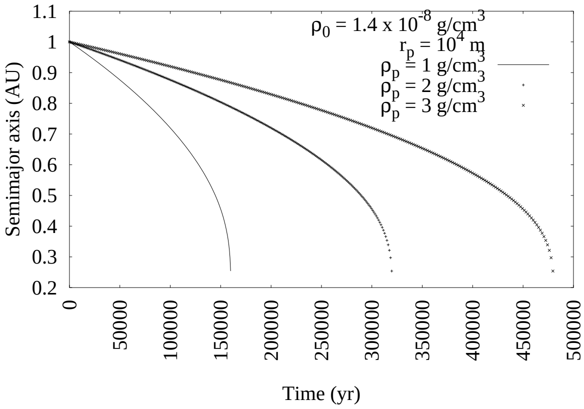


Figure 14: Semimajor axis versus time for bodies of radius $r_p = 10^4\,\mathrm{m}$ in a nebula with $\rho_0 = 10^{-8}\,\mathrm{g/cm^3}$.

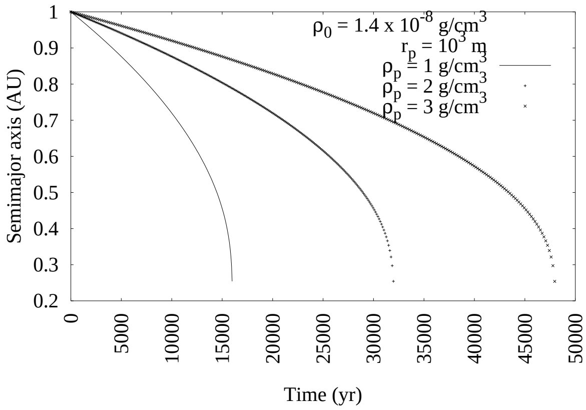


Figure 13: Semimajor axis versus time for bodies of radius $r_p = 10^3\,\mathrm{m}$ in a nebula with $\rho_0 = 10^{-8}\,\mathrm{g/cm^3}$.

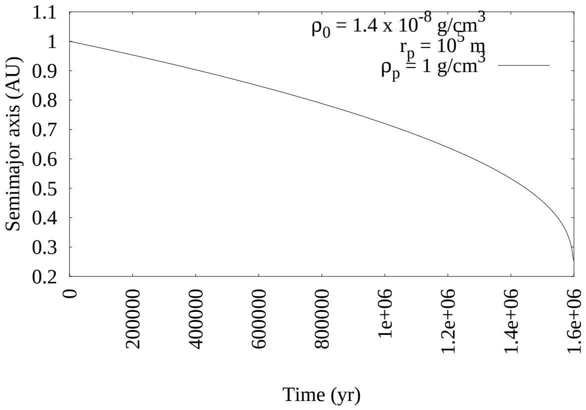


Figure 15: Semimajor axis versus time for bodies of radius $r_p = 10^5\,\mathrm{m}$ in a nebula with $\rho_0 = 10^{-8}\,\mathrm{g/cm^3}$.

## 5 Future Work

Thus far we have limited our studies to bodies initialized at 1 AU from the Sun on orbits with no eccentricity or inclination. In the future, we should extend the parameter space of interest to include bodies farther from the Sun and on eccentric and/or inclined orbits. In the latter case, Adachi et al. have predicted that such orbits should be circularized on a time scale that is very small compared with the decay time of the semimajor axis [6]. Although the results of preliminary simulations have agreed with this predicition, a more thorough analysis is required before we can make any general conclusions.

A more interesting problem that our solar nebula code will allow us to study is the effect of gas drag on resonance trapping in the solar system. This would involve adding a Jupiter-like body to the system and following the evolution of bodies placed in or near resonance with it. Such a study would allow us to determine more accurately the nature of resonance trapping in the early solar system and predict its effects on the orbital stability of various bodies.

## References

[1] B. Sicardy. Extra-solar planets. In *Solar System Formation and Evolution*, volume 149 of *Astronomical Society of the Pacific Conference Series*, pages 13–25, 1998.

[2] Jack J. Lissauer. Formation of planetary systems. In *Solar System Formation and Evolution*, volume 149 of *Astronomical Society of the Pacific Conference Series*, pages 1–11, 1998.

[3] D. C. Richardson, G. Lake, T. Quinn, and J. Stadel. Direct simulation of planet formation with a million planetesimals: A progress report. *American Astronomical Society Meeting*, 191:12811+, December 1997.

[4] D. C. Richardson, T. Quinn, J. Stadel, and G. Lake. Direct simulation of planet formation with a million planetesimals: First results. *AAS/Division of Planetary Sciences Meeting*, 30:2113+, September 1998.

[5] T. Kusaka, T. Nakano, and C. Hayashi. Growth of solid particles in the primordial solar nebula. *Progress in Theoretical Physics*, 44:1580–1595, 1970.

[6] I. Adachi, C. Hayashi, and K. Nakazawa. The gas drag effect on the elliptical motion of a solid body in the primordial solar nebula. *Progress in Theoretical Physics*, 56:1756–1771, 1976.

[7] C. Hayashi. Structure of the solar nebula, growth and decay of magnetic fields and effects of magnetic and turbulent viscosities on the nebula. *Progress in Theoretical Physics*, 70:35–53, 1981.

[8] H. Takeda, T. Matsuda, K. Sawada, and C. Hayashi. Drag on a gravitating sphere moving through gas. *Progress in Theoretical Physics*, 74:272–287, 1985.

[9] S. Ida and D. N. C. Lin. Long term gas drag effect on the structure of the asteroid belt and its implications for the solar nebula. *Astronomical Journal*, 112:1239+, September 1996.

[10] M. Lecar and F. Franklin. The solar nebula, secular resonances, gas drag, and the asteroid belt. *Icarus*, 129:134–146, September 1997.